

A New Compact Filter-Antenna for Modern Wireless Communication Systems

Wei-Jun Wu, Ying-Zeng Yin, Shao-Li Zuo, Zhi-Ya Zhang, and Jiao-Jiao Xie

Abstract—Design, fabrication, and measurement of a new compact filter-antenna for modern wireless communication systems are presented in this letter. Two microstrip square open-loop resonators, a coupled line, and a Γ -shaped antenna are used and integrated to be a filter-antenna. The Γ -shaped antenna is excited by a coupled line that is treated as the admittance inverter in filter design. The Γ -shaped antenna performs not only a radiator, but also the last resonator of the bandpass filter. Therefore, near-zero transition loss is achieved between the filter and the antenna. The design procedure follows the circuit approach—synthesis of bandpass filters. Measured results show that the filter-antenna achieves an impedance bandwidth of 16.3% (over 2.26–2.66 GHz) at a reflection coefficient $|S_{11}| < -10$ dB and has a gain of 2.41 dBi.

Index Terms—Filter-antenna, Γ -shaped antenna, open-loop resonator filter, synthesis.

I. INTRODUCTION

THE WIRELESS communication field has been experiencing a revolutionary growth in the last few decades. This has been caused by the invention of many wireless products and services such as wireless local area network, Global Positioning System (GPS), mobile phone, Bluetooth, etc. In these systems, both antennas and filters are usually larger components compared to other components. Thus, it will be of great interest if a single compact module can be designed to provide both the desired filtering and radiating performances.

There have been several efforts in the literature for integrating the filter and the antenna into a single module [1]–[7]. In [1], the design of the filter and the antenna was essentially independent. The direct connection of the filter and the antenna usually causes an impedance mismatch and deteriorates the filter's performance, especially near the band edges. To avoid this, an extra impedance transformation structure was used in between the filter and the antenna [2], [3]. However, the transition structure increases the complexity of the overall system, together with its weight, size, and losses. Recently, a co-design approach has been proposed to incorporate the filter and the antenna [4]–[7]. This integration approach reduces the filter-antenna size and the transition loss between the filter and the antenna. However,

Manuscript received July 20, 2011; revised September 21, 2011; accepted October 02, 2011. Date of publication October 13, 2011; date of current version October 24, 2011.

The authors are with the National Key Laboratory of Antenna and Microwave Technology, Xidian University, Xi'an 710071, China (e-mail: wj1218wu@126.com).

Color versions of one or more of the figures in this letter are available online at <http://ieeexplore.ieee.org>.

Digital Object Identifier 10.1109/LAWP.2011.2171469

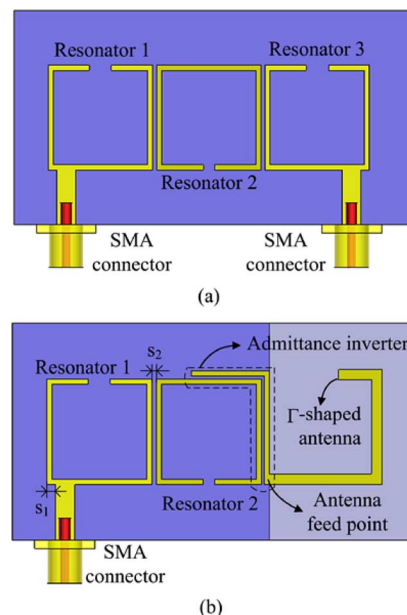


Fig. 1. (a) Microstrip three-pole filter. (b) Integrated three-pole filter-antenna.

the filter-antennas in [4] and [5] did not show good filter performance—especially the band-edge selectivity and stopband suppression and the admittance inverters of the filter-antennas in [6] and [7] were difficult to synthesize.

In this letter, a new compact three-pole filter-antenna for modern wireless communication systems is presented. Using the synthesis approach, two microstrip square open-loop resonators, a coupled line, and a Γ -shaped antenna are integrated to be a filter-antenna. Near-zero transition loss is achieved between the filter and the antenna. The total loss of the filter-antenna is almost identical to the filter insertion loss alone. The proposed filter-antenna has a small size of $0.41\lambda_g \times 0.6\lambda_g$, where λ_g is the guiding wavelength at 2.45 GHz. The planar structure of the filter-antenna is easy to fabricate and integrate with the circuit board of wireless communication systems. The filter-antenna supplies good skirt selectivity as the conventional bandpass filter, flat antenna gain in the passband, and high suppression in the stopband. The measured results show good agreement with the simulated ones.

II. FILTER SYNTHESIS

Before the integrated filter-antenna is designed, a reference three-pole microstrip square open-loop resonator filter is synthesized as shown in Fig. 1(a). Then, a three-pole filter-antenna is realized by replacing the third resonator of the filter with a Γ -shaped antenna as shown in Fig. 1(b).

A three-pole Chebyshev bandpass filter with a 0.1-dB equal-ripple and a fractional bandwidth (FBW) of 13% at 2.45 GHz is designed using standard filter synthesis techniques [8]. The coupling coefficients between resonators and the external quality factors of the resonators at the input and output port are $k_{12} = k_{23} = 0.12$ and $Q_{\text{ext},1} = Q_{\text{ext},2} = 7.93$. This filter consists of three open-loop resonators and is printed on a substrate with dielectric constant $\epsilon_r = 2.65$ and 0.6 mm thickness.

The external quality factor is obtained for the external resonator when it is loaded only by the external circuit, that is to say, the external quality factor obtained for the external resonator after eliminating the other resonators. The quality factor value can be adjusted by changing s_1 . A small external quality factor occurs at a small s_1 . The method used for the characterization of $Q_{\text{ext},1/2}$ as a function of s_1 is based on

$$Q_{\text{ext},1/2} = \frac{f_0}{\Delta f_{\pm 90^\circ}} \quad (1)$$

where $\Delta f_{\pm 90^\circ}$ represents the difference between the frequencies for which the phase of S_{11} is 90° higher and 90° lower than the phase of S_{11} in resonance [9]. The relationship between $Q_{\text{ext},1/2}$ and s_1 is obtained through simulations of the referred S_{11} parameter, in magnitude and phase. The variables of (1) are determined for each simulated value of s_1 as follows: f_0 is the frequency where the minimum S_{11} magnitude occurs, and $\Delta f_{\pm 90^\circ}$ can be readily calculated from the S_{11} phase response as indicated above, taking the phase of S_{11} in resonance as the phase corresponding to the frequency f_0 . Fig. 2(a) depicts the external quality factor variations as functions of s_1 . It is seen that the smaller the s_1 is, the smaller the external quality factor.

The coupling between the resonators is determined by the distance s_2 of the resonators. Stronger coupling occurs with a smaller s_2 . The characterization of $k_{12/23}$ is based on

$$k_{12/23} = \frac{1}{2} \left(\frac{f_{02}}{f_{01}} + \frac{f_{01}}{f_{02}} \right) \sqrt{\left(\frac{f_{p2}^2 - f_{p1}^2}{f_{p2}^2 + f_{p1}^2} \right)^2 - \left(\frac{f_{02}^2 - f_{01}^2}{f_{02}^2 + f_{01}^2} \right)^2} \quad (2)$$

where f_{01} and f_{02} are the self-resonance frequencies of each resonator, while f_{p1} and f_{p2} are the eigenfrequencies of the whole resonant structure [9]. Through electromagnetic simulation of each resonator, the self-resonance frequencies can be found. The eigenfrequencies are determined from simulations of the two coupled square open-loop resonators while changing the distance s_2 of the resonators. The curve $k_{12/23}$ versus s_2 is presented in Fig. 2(b). It is seen that the coupling coefficient decreases monolithically with the increase of s_2 .

III. INTEGRATED FILTER-ANTENNA SYNTHESIS

Fig. 3 shows the proposed filter-antenna, which contains two square open-loop resonators, a coupled line, and a Γ -shaped antenna. No intermediate transition structure is needed between the filter and the antenna in the proposed integration approach. Therefore, there is near-zero transition loss between the filter and the antenna. Since the antenna is to be designed in the filter

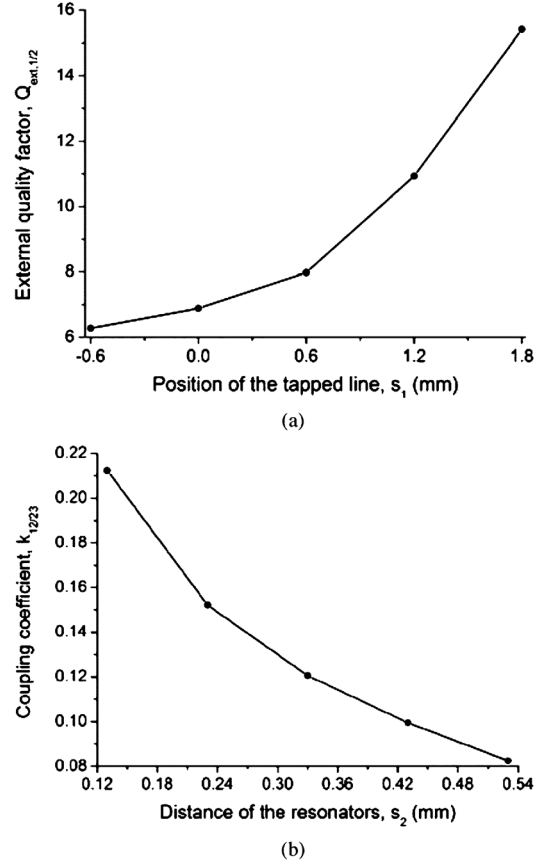


Fig. 2. Characterization curves for the two design parameters. (a) External quality factor $Q_{\text{ext},1/2}$. (b) Coupling coefficient $k_{12/23}$.

as the last resonator, the first step is to synthesize the quality factor of the antenna, Q_A , which can be extracted using [10]

$$Q_A = \frac{\omega_0}{2\text{Re}(Z_{\text{in}}(\omega_0))} \left. \frac{d(\text{Im}(Z_{\text{in}}))}{d\omega} \right|_{\omega = \omega_0} \quad (3)$$

where Z_{in} is the input impedance of the structure at the antenna feed point looking toward the antenna shown in Fig. 1(b). The ground plane of the antenna, which is also the ground plane of the circuitry, has a fixed size of $L \times W = 30 \times 30 \text{ mm}^2$. The resonant frequency of the antenna is defined by the total length ($x_1 + x_2 + x_3$) of the Γ -shape, which is 28.9 mm and is approximately a quarter-wavelength for 2.45 GHz. As shown in Fig. 4, Q_A is dependent on the horizontal strip length x_1 due to the strongest current distribution on this strip. This figure can be used as the design chart for synthesis of the parameter. Finally, x_1 , x_2 , and x_3 are selected to be 13, 12.1, and 3.8 mm, respectively, to realize $Q_A = Q_{\text{ext},2} = 7.93$.

In order to connect the Γ -shaped antenna to the second square open-loop resonator, a coupled line as admittance inverter is used. The length ($y_1 + y_2$) of the coupled line is nearly equal to $\lambda_g/4$ at 2.45 GHz. One line of the coupled line is the section of the second square open-loop resonator. The coupled line is designed as [11]. Consider a coupled line with even- and odd-mode characteristic impedances Z_{0e} and Z_{0o} , respectively, as shown in Fig. 5(a), which is to be equivalent to the circuit shown in Fig. 5(b) at 2.45 GHz. To have the same circuit performances

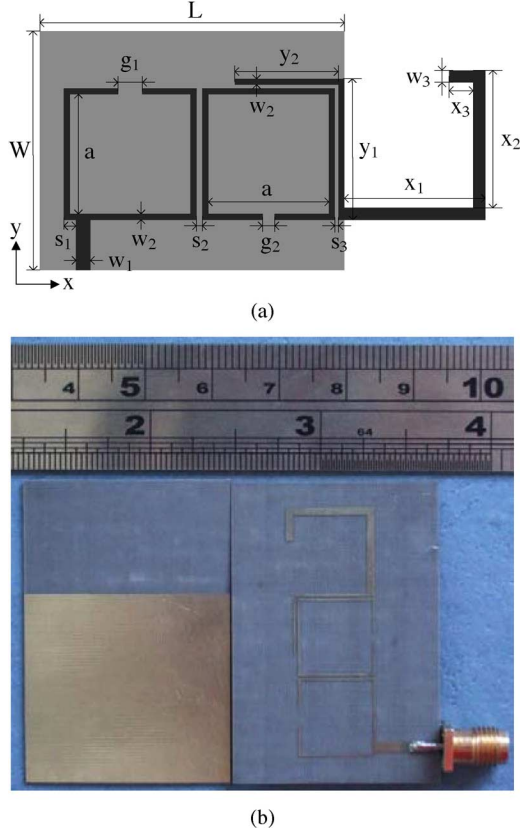


Fig. 3. Geometry of the proposed filter-antenna. (a) Top view ($W = 30$; $L = 30$; $w_1 = 1.64$; $s_1 = 0.6$; $a = 10.68$; $g_1 = 2.6$; $w_2 = 0.51$; $g_2 = 1.3$; $s_2 = 0.33$; $s_3 = 0.19$; $y_1 = 12.4$; $y_2 = 8.6$; $x_1 = 13$; $x_2 = 12.1$; $x_3 = 3.8$; $w_3 = 1.2$). All dimensions are in millimeters. (b) Photograph of the filter-antenna.

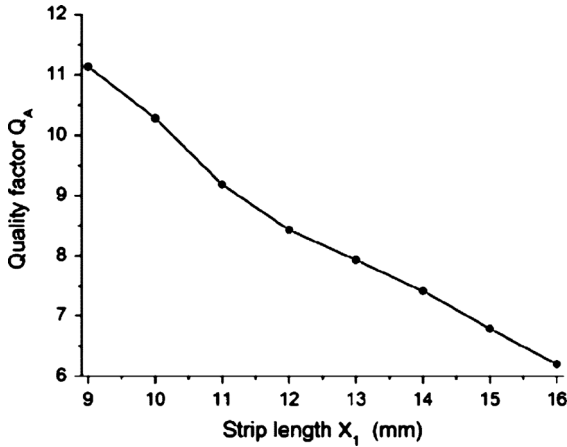


Fig. 4. Quality factor Q_A as a function of the strip length x_1 . $w_3 = 1.2$ mm, $x_1 + x_2 + x_3 = 28.9$ mm.

at 2.45 GHz, the ABCD matrices of the coupled line and the equivalent circuit should be equal at $\theta = \pi/2$, resulting into

$$Z_{0e}/Z_0 = 1 + J_{23}Z_0 + (J_{23}Z_0)^2 \quad (4a)$$

$$Z_{0o}/Z_0 = 1 + J_{23}Z_0 + (J_{23}Z_0)^2. \quad (4b)$$

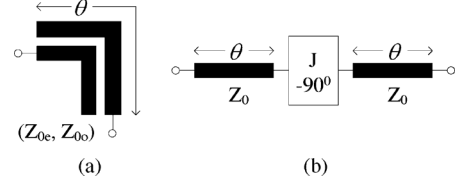


Fig. 5. (a) Geometry of the coupled line and (b) the corresponding equivalent circuit.

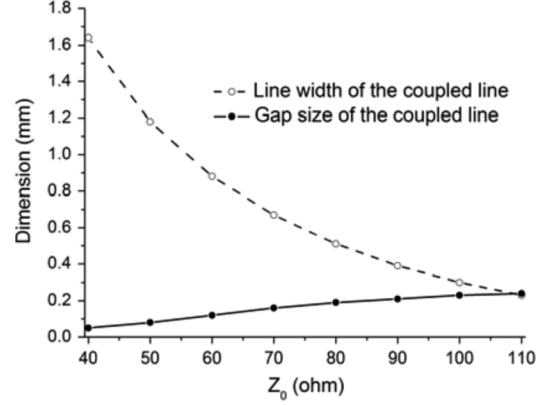


Fig. 6. Dimensions of the coupled line for different Z_0 in the proposed filter-antenna.

Therefore, once $J_{23}Z_0$ is known, the impedances and thus the dimensions of the coupled line can be obtained. The characterization of $J_{23}Z_0$ is based on

$$J_{23}Z_0 = 2\text{FBW}\theta/\sqrt{p_2p_3} \quad (5)$$

where FBW is the fractional bandwidth of the filter. θ is the coupled-line electrical length at 2.45 GHz. p_2 and p_3 are the element values of the low-pass prototype filter [9]. For this design, we have $p_2 = 1.1474$ and $p_3 = 1.0315$.

The even- and odd-mode characteristic impedances Z_{0e} and Z_{0o} can be calculated by using (4) and (5), respectively, from which the line width and the gap between lines are obtained. Note that these dimensions are dependent on the characteristic impedance Z_0 used in the synthesis of the filter-antenna. Fig. 6 depicts their variations as the functions of Z_0 . It is seen that the smaller the impedance Z_0 is, the smaller the gap size. When $Z_0 < 50\Omega$, the gap would become smaller than 0.1 mm, which is difficult to realize. Thus, for easy fabrication, a characteristic impedance of $Z_0 = 80\Omega$ is selected here. This would correspond to an inverter constant $J_{23}Z_0 = 0.3754$ and even- and odd-mode characteristic impedances $(Z_{0e}, Z_{0o}) = (121.31\Omega, 61.24\Omega)$. The line width w_2 and the gap s_3 between lines are equal to 0.51 and 0.19 mm.

IV. SIMULATED AND MEASURED RESULTS

The measured S_{11} and gain of the filter-antenna are compared to simulated results in Fig. 7. The measured S_{11} is below -25 dB across the entire bandwidth. The measured bandwidth of 16.3% is close to the simulated bandwidth of 14%. The 0.4% difference between the measured and simulated resonant frequencies—i.e., 2.46 and 2.45 GHz, respectively—is mainly due

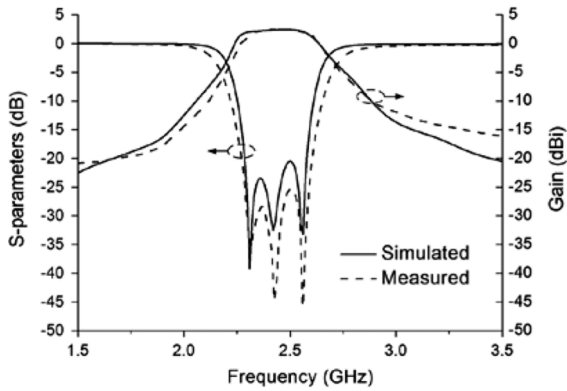


Fig. 7. Simulated and measured S_{11} and gain of the proposed filter-antenna.

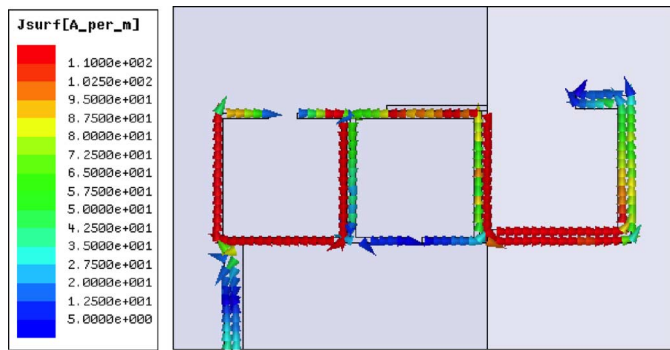


Fig. 8. Surface current distributions of the proposed filter-antenna at 2.45 GHz.

to the loss tangent of the substrate and the fabrication tolerances. The measured gain is 2.41 dBi at 2.45 GHz, which is very close to the simulated 2.53 dBi.

In order to study the radiation property of the proposed filter-antenna, surface current distributions of the filter-antenna at 2.45 GHz are given in Fig. 8. It can be noticed that the currents flow through the Γ -shaped antenna without changing the direction, and the strongest currents are distributed on the long horizontal strip. This indicates that the filter-antenna can obtain nearly omnidirectional radiation pattern in the yz -plane.

The measured and simulated total-field radiation patterns at 2.45 GHz in the xy - and yz -planes are presented in Fig. 9. The radiation pattern in the yz -plane is nearly omnidirectional with peak gain of 1.31 dBi.

V. CONCLUSION

A new compact third-order filter-antenna is proposed. A quarter-wavelength coupled line is used to integrate the Γ -shaped antenna and the microstrip filter resonators, given that the Γ -shaped antenna containing the radiating element is

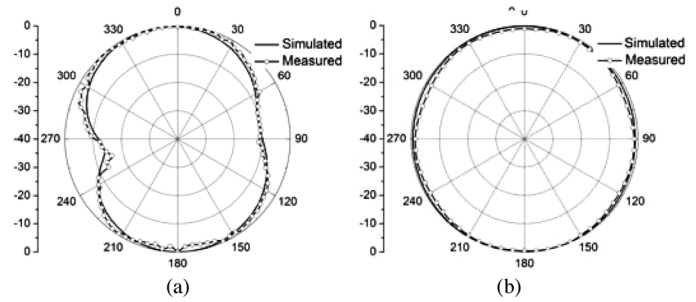


Fig. 9. Simulated and measured radiation patterns of the proposed filter-antenna. (a) xy -plane. (b) yz -plane.

one of the filter resonators. The proposed filter-antenna provides good skirt selectivity as the conventional bandpass filter, flat antenna gain in the passband, and high suppression in the stopband. The electrical response of the filter-antenna presents integrated filtering and radiating functions without damaging any of them. Owing to these results, the filter-antenna is very suitable for use in the RF front end that is essential for modern wireless communication systems.

REFERENCES

- [1] G. Goussetis and D. Budimir, "Antenna filter for modern wireless systems," in *Proc. 32nd Eur. Microw. Conf.*, 2002, pp. 1–3.
- [2] M. Troubat, S. Bila, M. Thévenot, D. Baillargeat, T. Monédière, S. Verdeyme, and B. Jecko, "Mutual synthesis of combined microwave circuits applied to the design of a filter-antenna subsystem," *IEEE Trans. Microw. Theory Tech.*, vol. 55, no. 6, pp. 1182–1189, Jun. 2007.
- [3] J. H. Lee, N. Kidara, S. Pinel, J. Laskar, and M. Tentzeris, "Fully integrated passive front-end solutions for a V-band LTCC wireless system," *IEEE Antennas Wireless Propag. Lett.*, vol. 6, pp. 285–288, 2007.
- [4] O. A. Nova, J. C. Bohórquez, N. M. Peña, G. E. Bridges, L. Shafai, and C. Shafai, "Filter-antenna module using substrate integrated waveguide cavities," *IEEE Antennas Wireless Propag. Lett.*, vol. 10, pp. 59–62, 2011.
- [5] J. H. Zuo, X. W. Chen, G. R. Han, L. Li, and W. M. Zhang, "An integrated approach to RF antenna-filter co-design," *IEEE Antennas Wireless Propag. Lett.*, vol. 8, pp. 141–144, 2009.
- [6] C. K. Lin and S. J. Chung, "A compact filtering microstrip antenna with quasi-elliptic broadside antenna gain response," *IEEE Antennas Wireless Propag. Lett.*, vol. 10, pp. 381–384, 2011.
- [7] C. K. Lin and S. J. Chung, "A compact edge-fed filtering microstrip antenna with 0.2 dB equal-ripple response," in *Proc. 39th Eur. Microw. Conf.*, 2009, pp. 378–380.
- [8] R. J. Cameron, "General coupling matrix synthesis methods for Chebyshev filtering functions," *IEEE Trans. Microw. Theory Tech.*, vol. 47, no. 4, pp. 433–442, Apr. 1999.
- [9] J. S. Hong and M. J. Lancaster, *Microstrip Filters for RF/Microwave Applications*. New York: Wiley, 2001.
- [10] Y. Yusuf and X. Gong, "Compact low-loss integration of high-Q 3-D filters with highly efficient antennas," *IEEE Trans. Microw. Theory Tech.*, vol. 49, no. 4, pp. 857–865, Apr. 2011.
- [11] S. B. Cohn, "Parallel-coupled transmission-line-resonator filter," *IEEE Trans. Microw. Theory Tech.*, vol. MTT-6, no. 2, pp. 223–231, Apr. 1958.